Patterns of crossover distribution in *Drosophila mauritiana* necessitate a re-thinking of the centromere effect on crossing over

R. Scott Hawley,[1] Andrew Price,[1] Hua Li,[1] Madhav Jagannathan [ID],[2] Cynthia Staber,[1] Stacie E. Hughes,[1,*]
Stefanie Williams [ID],[1] Anoja Perera,[1] Rhonda R. Egidy,[1] Amanda Lawlor,[1] Danny E. Miller,[3,4] Justin P. Blumenstiel [ID] [5,*]

[1]Stowers Institute for Medical Research, Kansas City, MO 64110, USA
[2]Institute of Biochemistry, Department of Biology, ETH Zürich, 8093 Zürich, Switzerland
[3]Division of Genetic Medicine, Department of Pediatrics, University of Washington, Seattle, WA 98105, USA
[4]Department of Laboratory Medicine and Pathology, University of Washington and Seattle Children's Hospital, Seattle, WA 98105, USA
[5]Department of Ecology and Evolutionary Biology, University of Kansas, Lawrence, KS 66045, USA

*Corresponding author: Stowers Institute for Medical Research, 1000 E 50th Street, Kansas City, MO 64110, USA. Email: sfh@stowers.org; *Corresponding author:
Department of Ecology and Evolutionary Biology, University of Kansas, 1200 Sunnyside Avenue, Lawrence, KS 66045, USA. Email: jblumens@ku.edu

We present an SNP-based crossover map for *Drosophila mauritiana*. Using females derived by crossing 2 different strains of *D. mauritiana*, we analyzed crossing over on all 5 major chromosome arms. Analysis of 105 male progeny allowed us to identify 327 crossover chromatids bearing single, double, or triple crossover events, representing 398 crossover events. We mapped the crossovers along these 5 chromosome arms using a genome sequence map that includes the euchromatin-heterochromatin boundary. Confirming previous studies, we show that the overall crossover frequency in *D. mauritiana* is higher than is seen in *Drosophila melanogaster*. Much of the increase in exchange frequency in *D. mauritiana* is due to a greatly diminished centromere effect. Using larval neuroblast metaphases from *D. mauritiana*— *D. melanogaster* hybrids we show that the lengths of the pericentromeric heterochromatin do not differ substantially between the species, and thus cannot explain the observed differences in crossover distribution. Using a new and robust maximum likelihood estimation tool for obtaining Weinstein tetrad distributions, we observed an increase in bivalents with 2 or more crossovers when compared with *D. melanogaster*. This increase in crossing over along the arms of *D. mauritiana* likely reflects an expansion of the crossover-available euchromatin caused by a difference in the strength of the centromere effect. The crossover pattern in *D. mauritiana* conflicts with the commonly accepted view of centromeres as strong polar suppressors of exchange (whose intensity is buffered by sequence nonspecific heterochromatin) and demonstrates the importance of expanding such studies into other species of Drosophila.

Keywords: meiosis; crossover patterning; centromere effect; crossover map; *D. mauritiana*; Weinstein tetrad analysis; FlyBase

Introduction

Genetics functions best as a comparative science—Kenneth W. Cooper

Since its discovery over a century ago in *Drosophila melanogaster*, crossing over has been the subject of extensive study in both meiotic biology and Drosophila genetics. One of the most active areas of that research focuses on determining the factors and mechanisms that control the number of crossover events and their distribution (Lindsley and Sandler 1977). We seek to understand the *cis*- and *trans*-acting elements that control the number and distribution of crossovers, as well as those mechanisms that mediate such processes as crossover assurance (Pazhayam *et al.* 2021) and crossover interference (Sturtevant 1913, 1915; Berchowitz and Copenhaver 2010). Our goal is to use this knowledge to elucidate the genetic basis for the regional variation in crossover frequencies in the euchromatin (Lindsley and Sandler 1977; Szauter 1984) both within a given

genome and between species. Long-standing dogma suggests that such control could be exerted both by the existence of *trans*-acting factors that act on a genome-wide basis as well as *cis*-acting processes, such as polar exchange suppression exhibited by centromeres and telomeres.

Several approaches have been employed to understand variation in crossover rates between *D. melanogaster* and closely related species. First, mapping studies in *Drosophila simulans* that used visible markers suggested that the genetic map of *D. simulans* is approximately 30% longer than that of *D. melanogaster* (Sturtevant 1913, 1915; Barker and Moth 2001). Second, True *et al.* (1996) measured crossover rates in *Drosophila mauritiana* by using a large collection of marked transposon insertions in *D. mauritiana*. The position of these insertions was precisely determined by in situ hybridization to salivary gland polytene chromosomes to create crossover maps. The crossover frequencies

between pairs of these insertions were determined with 2-factor crosses and sets of adjacent intervals were summed to determine the distance from any given insertion to the most proximal insertion. For *D. melanogaster* and *D. simulans,* the recombination frequency between a given site and the base of the arm was obtained from standard reference maps. This effort allowed comparisons of the maps of these 3 species. Together, these studies demonstrated that the total map length of *D. mauritiana* was approximately 1.8 times that of *D. melanogaster*, while the total map length of *D. simulans* was estimated to be 1.3 times that of *D. melanogaster*. Surprisingly, the centromere-proximal regions of the euchromatin in *D. simulans* and *D. mauritiana* showed greater rates of crossing over when compared with *D. melanogaster*. This difference was not observed in more distal regions. Third, SNP-based maps of crossover distribution in *D. melanogaster* (Miller *et al.* 2016) and *Drosophia yakuba* (Pettie *et al.* 2022) have allowed more precise measurements of both crossover density along the 5 autosomal arms and the type of crossover recovered (single, double, or triple crossovers). Presgraves and collaborators have used a variety of tools to decipher the genetic basis for the observed differences in crossover rates in several species within the *melanogaster* species group (Cattani *et al.* 2012; Brand *et al.* 2018, 2019). They concluded that interspecies variation reflects the action of both *cis-* and *trans*-acting elements that determine crossover number and position.

The centromere effect: The suggestion by True *et al.* (1996) and Brand *et al.* (2018) that *cis*-acting elements, such as the centromeres, play a major role in creating interspecies variation in crossover number and distribution is intriguing. In *D. melanogaster*, the term "centromere effect" is used to describe a strong polar suppression of exchange generated by centromeres. (A brief history of the centromere effect is provided in the legend to Fig. 1.) Our current understanding of the centromere effect has been recently reviewed by the Sekelsky lab (Hartmann, Kohl, *et al.* 2019; Hartmann, Umbanhowar, *et al.* 2019; Pazhayam *et al.* 2021; Pazhayam, Frazier, *et al.* 2024), and so we present only a brief overview here. The centromere effect was first observed by Beadle (1932) following his analysis of exchange in translocation heterozygotes and then by Sturtevant and Beadle (1936) as part of their analysis of crossing over in *X* chromosome inversion homozygotes. Several subsequent studies both by Yamamoto and Miklos (1977, 1978) and by Hawley (1980) have supported the prevailing view that the centromere effect is generated by the centromeres themselves with its impact on euchromatin attenuated by the expanse of pericentromeric heterochromatin between the centromere and the euchromatin (see Fig. 1a).

Following Pazhayam, Frazier, *et al.* (2024), we should note that the absence of exchange within the satellite-rich heterochromatin itself is an intrinsic feature of centric heterochromatin presumably due to the fact that programed double-strand breaks (DSBs) in meiosis are precluded from these regions (Mehrotra and McKim 2006). Indeed, the current consensus is that the centromere effect reflects a polar suppression of crossing over in the centromere-proximal euchromatin, such that if these regions of euchromatin are moved distally from centric regions, they will regain the capacity to recombine at expected levels. It is proposed that the attenuation of recombination by pericentric heterochromatin is not by a special property of heterochromatin but is merely due to the increased physical distance between the centromere and euchromatin where crossing over occurs.

Several recent studies suggest that the centromere effect is partially under the genetic control of *trans*-acting factors. For example, the centromere effect is abrogated in *Drosophila* lacking
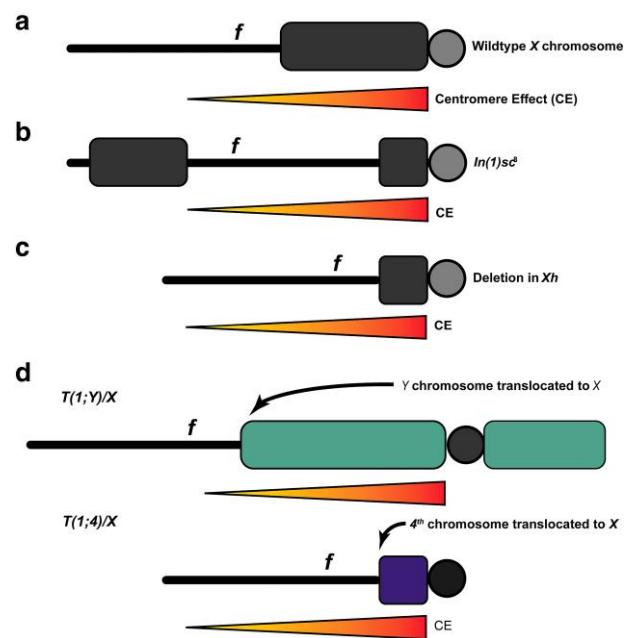

Fig. 1. The canonical view of the centromere effect. A schematic depiction of the canonical view of the centromere effect as defined by studies in *D. melanogaster*. Here the centromere effect is depicted as a polar suppression of recombination (orange triangles) emanating out from the centromeres (gray circles). Black lines represent the *X* chromosome euchromatin and dark gray boxes represent the *X* chromosome heterochromatin. The genetic locus *forked* (*f*) is shown for reference. a) The strength of the centromere effect on exchange in the euchromatin is thought to be attenuated by blocks of pericentromeric heterochromatin. b) As shown by Sturtevant and Beadle (1936), the movement of a large portion of the heterochromatin to a distal site by homozygous inversions allows the centromere effect to penetrate more deeply into the proximal euchromatin. c) Deleting proximal heterochromatin allows the centromere effect to spread further into the euchromatin (Schalet and LeFevre 1976; Yamamoto and Miklos 1977, 1978). d) *T(1;4)s* show much stronger centromere effects on exchange when heterozygous with a normal sequence *X* chromosome than do *T(1;Y)s* with similar breakpoints on the *X* chromosome. This was presumed to be a consequence of the ability of the larger blocks of heterochromatin on the *Y* chromosome to attenuate the centromere effect more effectively than the much smaller amount of heterochromatin on the *4th* chromosome (Hawley 1980). The *Y* chromosome heterochromatic sequences are represented in teal and the *4th* heterochromatic sequences are shown in purple.

the Bloom syndrome helicase (*Blm*) (Hatkevich *et al.* 2016). This has been proposed to arise from the induction of DSBs in regions proximal to the centromere being shunted from the Class I meiotic pathway, which would resolve as non-crossovers in proximal regions due to the centromere effect, into an alternate pathway of crossover resolution designated the Class II pathway that is insensitive to the centromere effect (Hatkevich *et al.* 2016). Variants of C(3)G, a transverse-filament protein of the synaptonemal complex (SC), also lead to increased amounts of recombination in proximal regions near the centromere (Billmyre *et al.* 2019). This suggests that the SC plays a role in the transmission of the centromere effect along the chromosome arm. Finally, mutations in *mei-218*, which has a crucial function in crossing over, lead to a change in the distribution of crossovers along the chromosome, with a greater proportion (though not greater number) of crossovers in centromere-proximal regions (Carpenter and Sandler 1974; Hartmann, Kohl, *et al.* 2019; Hartmann, Umbanhowar, *et al.* 2019; Pazhayam 2025). Modifying the extent and severity of the centromere effect via these *trans*-acting factors might be a strong driver of interspecies variation. This was shown by the work of Brand and colleagues (Brand *et al.* 2018, 2019) who provided

evidence that the rapid evolution of the *trans*-acting factor MEI-218 might be a component of intraspecific variation in the recombination rate by modulating the severity of the centromere effect. These authors showed that replacing the *D. melanogaster* mei-218 gene with a transgenic copy of its *D. mauritiana* ortholog resulted in an increase in crossing over, most notably in the proximal and distal euchromatin. Indeed, the authors suggest the different mei-218 genes in *D. melanogaster* and *D. mauritiana* control crossover distribution by "modulating the intensity of centromeric and telomeric suppression of crossing over." In other words, species-level differences arise from both the actions of *cis*-acting mechanisms, such as the centromere and telomere effects, and *trans*-acting factors such as the MEI-218 protein, which is thought to be a pro-crossover factor (Kohl *et al.* 2012; Brand *et al.* 2019; Hartmann, Kohl, *et al.* 2019; Hartmann, Umbanhowar, *et al.* 2019).

Here we extend this body of knowledge by providing an SNP-based map of crossing over in *D. mauritiana*. We confirm that the frequency of crossing over is increased in *D. mauritiana* compared with *D. melanogaster*. Our data confirm and extend the suggestion of True *et al.* (1996) that much of this increase can be ascribed to a greatly weakened centromere effect on all arms except 2L. This diminishment of the centromere effect increases the area in which crossovers can occur for 4 of the 5 chromosome arms in *D. mauritiana*. The diminishment of crossover suppression in proximal euchromatin, in the absence of obvious changes in the amount of centromeric heterochromatin, requires a reconsideration of our current understanding of the centromere effect. Instead of being fixed between species, the strength of the centromere effect may vary and this is likely to impact the evolution of global recombination rates.

Materials and methods
Fly stocks and husbandry
The following *D. mauritiana* wild-type lines were obtained from the National Drosophila Species Stock Center at Cornell University: Le Reduit, Mauritiana—14021-0241.150 (Mau_LR), Mauritiana 2—14021-0241.05 (Mau_2), Mauritiana 3—14021-0241.08 (Mau_3), and Mauritiana genome line—14021-0241.151 (Mau_G). *D. mauritiana* stocks were maintained on a 12-h light/dark cycle on standard laboratory molasses food at 25°C with ~40% humidity.

Husbandry for the D. mauritiana—D. melanogaster hybrid: All fly stocks were raised on standard Bloomington medium at 25°C. *D. melanogaster y w* and *D. mauritiana w^1* (DSSC#14021-0241.60) were used for the mitotic chromosome spreads.

DNA preparation and sequencing of parental lines
Genomic DNA from several strains of *D. mauritiana*, including the 2 strains used for the mapping studies, was isolated from 20 females (2 × 10 flies/prep) from each line using the Maxwell 16 Tissue DNA purification kit on the Maxwell 16 instrument (Promega). Samples were eluted in 300 µl water containing RNase A at 20 mg/ml. Like samples were combined, extracted once with phenol/chloroform, and precipitated at −20°C. Samples were resuspended in 22 µl of ultrapure water and quantitated on a Qubit fluorometer (Thermo Fisher Scientific). DNA-seq libraries were generated from 500 ng of DNA. The libraries were made according to the manufacturer's directions for the Illumina DNA Library Prep, (M) Tagmentation (Illumina, Cat. No. 20060060) and Nextera DNA UD Indexes (set A) (Illumina, Cat. No. 20018704) with 5 cycles of PCR. The resulting short fragment libraries were checked for quality and quantity using the Bioanalyzer (Agilent) and Qubit 2.0 Fluorometer (Thermo Fisher Scientific). The libraries were pooled and sequenced as 100 bp paired reads on a P2 flow cell using the Illumina NextSeq 2000 instrument. Following sequencing, Illumina Primary Analysis version NextSeq2K RTA 3.9.2 and bcl-convert-3.10.5 were run to demultiplex reads for all libraries and generate FASTQ files.

After sequencing, raw fastq files were adapter trimmed using Trim Galore (v0.6.10) and aligned to the *D. mauritiana* reference genome (D_mauritiana_ASM438214v1; RefSeq) using bwa mem (v0.7.17). Aligned reads were then deduplicated by processing them through samtools (v1.18) fixmate, sort, and markdup with the -r argument. Variant calling was run on these deduplicated reads using deepvariant (v1.5.0) with the Whole Genome Sequence model type argument. SNPs detected by deepvariant were filtered by vcftools (v0.0.16) to only retain biallelic, substitution point mutations with a minimum genotype quality of 20. A list of line-specific parental mutations was generated by comparing the filtered variant calls from the 3 parental samples and dropping identical shared mutations.

DNA preparation, sequencing, alignment, and SNP calling of individual flies
Among pairwise comparisons, the Mauritiana 2 (Mau_2) and the Mauritiana genome line (Mau_G) were determined to have the largest number of unshared single-nucleotide variants (i.e. found in Mau_2 but not Mau-G and vice versa) across any pair of parental lines and the broadest distribution across the genome (Supplementary Fig. 1). We then used Mau_G and Mau_2 heterozygotes for the recombination studies presented below. Mau_2 virgin females were mated to Mau_G males to produce heterozygous female progeny (denoted as 2-G in the sequence file name, see below). Heterozygous virgin female progeny were then mated individually to Mau_LR, Mau_G, or Mau_2 males to produce male progeny bearing 1 copy of each maternal, potentially recombinant, chromosome. We used different male genotypes depending on their experimental availability as some cross combinations were poorly fertile (Garrigan *et al.* 2014). Use of different male genotypes for backcrossing is not expected to influence results since crossing over occurs in females and the bioinformatics pipeline for crossover detection was easily adapted to each male genotype. Crosses between F1 females and Mau_LR males were designated as outcrosses. Crosses between F1 females and either Mau_2 or Mau_G males were designated as backcrosses.

A total of 108 individual male progeny were obtained from all the crosses: 69 of those progeny were obtained from the outcross to Mau_LR males, 25 from the backcross to Mau_2 males, and 14 from the backcross to Mau_G males. These males were starved for 4–6 h and frozen for downstream analysis. Sequence was successfully obtained from 105 males.

Genomic DNA was extracted from individual frozen males using the Qiagen DNeasy Blood and Tissue Kit (Qiagen #69506) with the following modifications. Single flies were homogenized using a pestle (Kimble #749520-0090 or similar) with a handheld homogenizer (VWR 47747-370) in 180 µl of ATL buffer, after which 4 µl of RNase A [100 mg/ml] was added. All other steps followed the standard manufacturer's protocol, except DNA was eluted in 2 × 50 µl of 10 mM Tris (pH 8.0). The DNA eluate was then concentrated to ~50 µl by centrifugation in Microcon DNA Fast Flow centrifugal filters (Merck Millipore, MRCFOR100) to achieve an average yield of 112 ng/fly. DNA was quantified using a Qubit fluorometer. Individual males were labeled to identify the father, the heterozygous mother, and sibling number. Thus, xG_13.2 was the second male isolated from female 13 mated to a Mau_G father. At least 3 sibling males were collected from each cross. Numbers may not be sequential because not all preps yielded sufficient DNA for sequencing.

Initially, DNA-Seq libraries were generated for 12 samples from 20 ng of genomic DNA, as assessed using the Qubit 2.0 Fluorometer, according to the manufacturer's directions with 15 minutes of enzymatic fragmentation at 37°C, targeting 200–450 bp, followed by a 10-fold dilution of the universal adaptor and 6 cycles of PCR with the NEBNext Ultra II FS DNA Library Prep Kit for Illumina (NEB, Cat. No. E7805S), and the NEBNext Multiplex Oligos for Illumina (96 Unique Dual Index Primer Pairs) (NEB, Cat. No. E6440S) and purified using the SPRIselect bead-based reagent (Beckman Coulter, Cat. No. B23318). Resulting short fragment libraries were checked for quality and quantity using the Bioanalyzer (Agilent) and Qubit 2.0 Fluorometer. Equal molar libraries were pooled, quantified, and sequenced on a Mid-Output flow cell of an Illumina NextSeq 500 instrument using NextSeq Control Software 4.0.1 with the following read length: 8 bp Index1, 151 bp Read1, 151 Read2, and 8 bp Index2. Following sequencing, Illumina Primary Analysis version NextSeq RTA 2.11.3.0 and bcl-convert-3.10.5 were run to demultiplex reads for all libraries and generate FASTQ files. Subsequently, additional DNA from the same 12 samples was prepared in duplicate using 1/10th reaction volumes, 1:30 fold adapter dilutions, and 8 cycles of PCR with the same reagents and conditions.

The additional 93 samples used in the analysis were prepared using the Seqwell plexWell 96 library prep. DNA-seq libraries were generated from 6.5–16 ng of DNA, as assessed using the Qubit Fluorometer. The libraries were made according to the manufacturer's directions for the seqWell purePlex DNA Library Prep Kit for Illumina Sequencing Platforms (seqWell, Cat. No. 301067) with kit supplied Indexes (seqWell, Cat. No. 301067) with 8 cycles of PCR. The resulting short fragment libraries were checked for quality and quantity using the Bioanalyzer and Qubit 2.0 Fluorometer. Equal molar libraries were pooled, quantified, and converted to process on the Element Biosciences AVITI with the Element Adept Library Compatibility Workflow, following the Adept Rapid PCR-Free Protocol. The converted pool was sequenced on a 2 × 150 Cloudbreak High Output flow cell (Cat. No. 860-00003), using AVITI OS 2.3.0 with the following read length: 10 bp Index1, 10 bp Index2, 151 bp Read1, and 151 bp Read2. Following sequencing, Bases2Fastq was run to demultiplex reads for all libraries and generate FASTQ files. The sequencing depth of the offspring from both the original 12 and subsequent 93 offspring samples is represented in Supplementary Fig. 2.

Detection and validation of crossovers

A schematic of the crossover detection workflow is described in Supplementary Figs. 3 and 4. R (R 4.2.3) was used to process VCF files from individual offspring and identify candidate crossover events using parent-specific variants. The first step filters out the offspring vcf file to only retain variants that match the line-specific parental variant (private variants) list. Supplementary Table 1 provides the variants identified in the sequenced offspring that did not match the parental lines. These were apparently segregating in the parental lines and were not used to identify the location of crossovers. Each chromosome was then binned into non-overlapping 50 kb bins, summing the number of private variants (scored as either present or absent, irrespective of zygosity) belonging to each of the 3 parental lines in each bin. For each 50 kb bin, this provided a count for variants that are private to each of the 3 lines. Using these counts, 2 approaches were taken, depending on whether the cross was a backcross or an outcross. For offspring derived from the F1 by Mau_LR outcrosses, bins in the bottom 25 percentile of the total number of matched variants were dropped to decrease noise caused by low levels of variation. Crossovers were then detected by identifying bins where the proportion of total variants derived from 1 line

(either Mau_2 or Mau_G) flipped compared with the previous bin (Outcross detection method 1). For example, if 1 50-kb bin identified the presence of 195 variants from Mau_2 and 2 variants from Mau_G, and the subsequent bin identified the presence of only 3 variants from Mau_2, but 249 variants from Mau_G, this would indicate a crossover.

For the offspring of backcrosses to either Mau_G and Mau_2 (Backcross detection method 2), a different approach was taken. This is because, in contrast to the outcross detection method, a crossover is not simply identified when, across non-overlapping windows, there is a balanced "flip" in the counts of variants between the Mau_G and Mau_2 lines. Instead, a crossover is identified when the proportion of private variants identified from 1 line switches between approximately 50% (the heterozygous state of the 2 haplotypes) and either 0 or 100% (the homozygous state for one of the lines). For this procedure, bins with variant counts above the 95th percentile or below the 10th percentile of total SNPs matching the male parental line were removed to limit the impact of mapping artifacts. In addition to counting the number of private variants belonging to each parental line identified in each 50 kb bin, we also counted the number of Mau_2 and Mau_G private variants found in the 3 upstream and downstream bins. *k*-means clustering was applied on those 14 total features (current, upstream, and downstream Mau-G and Mau2 counts) to cluster each bin into 1 of 2 clusters. Crossovers were detected by finding bins where the 3 previous bins belong to 1 cluster and the 3 following bins belong to the other. Since all sequenced offspring were males, the X chromosome crossovers were found using outcross detection method 1 for all samples. All crossovers were validated visually in IGV (Robinson *et al.* 2011). Only 1 crossover event (a possible double crossover on *3L*) failed to validate in IGV. Crossover events were categorized into classes based on the number of crossovers observed per chromatid: zero or non-crossovers (NCOs), single crossovers (SCOs), double crossovers (DCOs), triple crossovers (TCOs), and quadruple crossovers (4COs).

The number of SNPs within the heterochromatic regions for the offspring is described in Supplementary Table 2.

Availability of sequence data

All sequences used in this study are publicly available at https://www.ncbi.nlm.nih.gov/sra/PRJNA1168080. The sample names for sequences posted identify the paternal strain used. For example, sample name 2-Gx2 refers to heterozygous female (Mau_2/Mau_G) crossed to Mau_2 males, sample name 2-GxG refers to heterozygous female (Mau_2/Mau_G) crossed to Mau_G males, and sample name 2-GxLR refers to heterozygous female (Mau_2/Mau_G) crossed to Mau_LR males. VCF files are provided in GSA FigShare https://doi.org/10.25386/genetics.28506611.

DNA fluorescence in situ hybridization

For mitotic chromosome spreads, larval 3rd instar brains were squashed according to previously described methods (Larracuente and Ferree 2015). Briefly, tissue was dissected into 0.5% sodium citrate for 5–10 min and fixed in 45% acetic acid/2.2% formaldehyde for 4–5 min. Fixed tissues were firmly squashed with a cover slip and slides were submerged in liquid nitrogen until bubbling ceased. Coverslips were then removed with a razor blade and slides were dehydrated in 100% ethanol for at least 5 min. After drying, hybridization mix (50% formamide, 2× SSC, 10% dextran sulfate, 100 ng of each probe) was applied directly to the slide, samples were heat denatured at 95°C for 5 min and allowed to hybridize overnight at room temperature. Following hybridization, slides were washed 3 times for 15 min in 0.2× SSC and mounted with VECTASHIELD with

DAPI (Vector Labs). The following satellite DNA probes were used for in situ hybridization: $(AAGAG)_6$, $(AATAACATAG)_3$ and AGGATTTAGGGAAATTAATTTTTGGATCAATTTTCGCATTTTTTG-TAAG (359 bp repeat) and have been previously described (Jagannathan *et al.* 2017). Fluorescent images were taken using a Leica TCS SP8 confocal microscope with 63× oil-immersion objectives (NA = 1.4). Brightfield images were acquired using a Keyence microscope. Images were processed using Adobe Photoshop software.

Maximum likelihood estimates of tetrad classes

The frequencies of tetrad classes, denoted as Er, estimate the number of tetrads with r crossovers, where E_0 corresponds to tetrads with no crossovers, E_1 to those with 1 crossover, E_2 to those with 2, and so on. Crossover events can be categorized based on the number of crossovers per chromatid. Let $X = (X_{nCO}, X_{sCO}, X_{dCO}, X_{tCO}, X_{qCO})$ represent the counts for zero crossover (nCO), single crossover (sCO), double crossovers (dCO), triple crossovers (tCO), and quadruple crossovers (qCO), respectively. Zwick *et al.* (1999) demonstrated that the distribution of crossover counts follows a multinominal distribution

$$(X_{nCO}, X_{sCO}, X_{dCO}, X_{tCO}, X_{qCO})$$
$$\sim Multinomial(N, (p_{nCO}, p_{sCO}, p_{dCO}, p_{tCO}, p_{qCO}))$$

Where p_{nco}, psc_o, p_{dco}, p_{tco}, and p_{qco} denote the probabilities associated with each crossover category, and N represents the total number of observed crossovers. Assuming that crossovers are randomly distributed along chromatids without interference, Weinstein (1936) demonstrated that each crossover class probability is a linear combination of the frequencies of tetrad classes, E_r. The likelihood function for the observed crossover events is given by:

$$L(X|p) = \frac{N!}{x_{nCO}! * x_{sCO}! * x_{dCO}! * x_{tCO}! * x_{qCO}!}(p_{nCO}^{nCO}p_{sCO}^{sCO}p_{dCO}^{dCO}p_{tCO}^{tCO}p_{qCO}^{qCO})$$

where

$$p_{nCO} = E_0 + \frac{E_0}{2} + \frac{E_1}{4} + \frac{E_2}{8} + \frac{E_3}{16}$$
$$p_{sCO} = \frac{E_1}{2} + \frac{E_2}{2} + E_3 * \frac{3}{8} + E_4 * \frac{4}{16}$$
$$p_{dCO} = \frac{E_2}{4} + E_3 * \frac{3}{8} + E_4 * \frac{6}{16}$$
$$p_{tCO} = \frac{E_3}{8} + E_4 * \frac{4}{16}$$
$$p_{qCO} = \frac{E_4}{16}$$

We employed optimization techniques to estimate the maximum likelihood estimates (MLEs) of E_rs. Specifically, the Nelder-Mead algorithm was utilized via the optim() function in R, with Weinstein's algebraic solutions serving as the initial parameter values. Additionally, the probabilities were constrained to be positive throughout the optimization process.

A public-facing web app for applying our MLE method on user-submitted crossover count data is available at https://simrcompbio.shinyapps.io/CrossoverMLE/. The app was created using R (v4.3.1) and shiny (v1.7.5) (https://CRAN.R-project.org/package=shiny) and hosted on shinyapps.io.

Results

Generation of the Mau_2/Mau_G heterozygous females: In order to choose the 2 *D. mauritiana* strains used to create the heterozygous females that we used for mapping crossovers, we sequenced 4 strains of *D. mauritiana* (Mau_G, Mau_2, Mau_3, and Mau_LR) and identified SNPs present in each line (Supplementary Fig. 1). SNPs were filtered using vcftools to only retain biallelic, substitution point mutations with a minimum genotype quality of 20. A list of line-specific parental mutations was generated by comparing the filtered variant calls from the parental samples and removing any identical shared mutations.

We chose to use the Mau_G and Mau_2 lines for our crosses. Mau_G and Mau_2 were chosen because they had the largest number of unshared variants (i.e. found in Mau_2 but not Mau_G and vice versa) across any pair of parental lines. The original analysis found 1,467,376 SNPs unique to 1 of the 2 lines, the most out of all possible pairwise comparisons of sequenced strains. The rationale being the more unique SNPs that exist between the parents, the more accurate our ability to position crossover sites.

We then performed single-fly sequencing of 105 individual male progeny from Mau_2/Mau_G heterozygous females. The average depth of sequencing for the initial 12 test samples was 21.42×, while the average depth of the subsequent 93 samples was 15.81×. Analysis of these males allowed us to evaluate crossover events on 5 chromosome arms (*X, 2L, 2R, 3L,* and *3R*) in each male, obtaining the CO positions for 525 arms. From this data, we identified 198 NCO arms, and 327 arms with 1 or more crossover events: 262 SCO-bearing arms, 59 DCO arms, and 6 TCO arms. Together, we mapped 398 crossover events (Table 1) and determined their precise position (Fig. 2). Because our data was relatively low coverage, we did not search for gene conversion events or assay for crossing over on the *4th* chromosome. With 15× coverage, a single heterozygous SNP from a given haplotype has about a 3 in 100,000 (0.5^{15}) chance of being sequenced with zero depth, which is expected to yield a significant challenge for detecting rare gene conversion events across the entire genome.

Species-relatedness: a comparison of the genomes; D. melanogaster and *D. mauritiana* are both members of the *melanogaster* species complex. (Supplementary Fig. 5). Their karyotypes and the maps of their salivary gland polytene chromosomes are identical, except for a large paracentric and euchromatic inversion on *3R*. Full genome sequence studies by Chakraborty *et al.* (2021) confirm the close relatedness adding only several small inversions on the X chromosome to the difference in euchromatic sequence. According to the canonical understanding of the centromere effect, if the pericentromeric regions of heterochromatin in *D. mauritiana* were substantially longer than those of *D. melanogaster,* that should decrease centromere-induced suppression of euchromatic crossing over in *D. mauritiana* compared with *D. melanogaster*. However, as shown below, there is no evidence for a substantial difference in the lengths of these regions between the 2 species.

Total map length comparison: Table 2 displays the total map length of each arm in *D. mauritiana* compared with the values obtained by Miller *et al.* (2016) for *D. melanogaster*, which used a similar sequencing approach for identifying crossovers. In sum, the total map length of *D. mauritiana* is 1.36 times greater than that observed for *D. melanogaster*. This increase is substantial, albeit lower than the 1.8-fold increase reported by True *et al.* (1996). This increase in map length is not uniform across the 5 arms. The map lengths of the *3R* and *3L* arms in *D. mauritiana* are increased 1.3 and 1.8 times, respectively, compared with their map lengths in *D. melanogaster,* while the map length of *2L* is increased by only a factor of 1.05. True *et al.* (1996) also found that the greatest increase in total map length was on the *3rd* chromosome (2.1 times) compared with *D. melanogaster* than on the X (1.8 times) or *2nd* chromosome (1.6 times) (True *et al.* 1996).

Table 1. Crossover progeny type recovered.

Crossover type	Chr 2L[a]	Chr 2R	Chr 3L	Chr 3R	Chr X
D. mauritiana (this paper N = 105)					
NCO	47.6 (50)	36.2 (38)	35.2 (37)	28.6 (30)	40.9 (43)
SCO	47.6 (50)	51.4 (54)	55.2 (58)	50.0 (53)	44.8 (47)
DCO	4.8 (5)	12.4 (13)	7.6 (8)	17.1 (18)	14.3 (15)
TCO	0.0 (0)	0.0 (0)	1.9 (2)	3.8 (4)	0.0 (0)
D. melanogaster (Miller *et al.* 2016. N = 196)					
NCO	52.5 (101)	51.5 (101)	49.4 (97)	50.5 (99)	49.5 (97)
SCO	44.9 (88)	45.9 (90)	42.8 (84)	43.9 (86)	43.9 (86)
DCO	2.5 (5)	2.5 (5)	7.6 (15)	5.1 (10)	6.6 (13)
TCO	0.0 (0)	0.0 (0)	0.0 (0)	0.5 (1)	0.0 (0)

[a]Number is percent of total flies of that class. Number in parentheses is the total number of flies of a given class.

Distribution of all crossover events: Fig. 3 presents the crossover density plots for each of the 5 arms in *D. mauritiana*. Similar plots based on the data from Miller *et al.* (2016) for *D. melanogaster* are presented for comparison. These plots also show the euchromatin-heterochromatin boundary and the position of a fixed euchromatic inversion on *3R* in *D. mauritiana*. The distribution of medial and distal crossover events in *D. mauritiana* does not appear different from that of *D. melanogaster* (see Fig. 3), even on *3R*. However, there is an obvious increased frequency of exchange in the proximal euchromatin of *D. mauritiana* when compared with *D. melanogaster*. To evaluate whether the increased map length of *D. mauritiana* could be attributed primarily to differences in proximal regions, we performed a statistical comparison with *D. melanogaster* across arm segments divided into thirds: distal, medial, and proximal (Table 3). We considered the total number of crossovers per segment irrespective of the physical distance of each segment, and also the number of crossovers in each segment normalized by physical distance.

Not accounting for physical distance, 4 (*2R*, *3L*, *3R*, and *X*) out of the 5 proximal regions showed significantly greater amounts of crossing over in *D. mauritiana*. Only 1 medial region, on *3L*, showed a significant difference, with *D. mauritiana* also displaying a higher crossover rate. The recombination frequency of 2 distal regions was significantly different, with one showing a higher recombination rate in *D. mauritiana* (*3R*) and the other showing the opposite pattern (*3L*). Accounting for physical distance, the results were essentially the same, with minor differences. In particular, the medial region of *2R* now showed a significantly higher per bp recombination rate in *D. mauritiana* and the distal region of *3L* no longer showed a significantly greater amount of recombination in *D. melanogaster*. Together, these results are most easily interpreted as a decrease in the ability of the centromere effect to reduce the frequency of crossing over in the proximal euchromatin of *D. mauritiana* present on 4 arms of *D. mauritiana*.

Dissimilarities between the crossover distributions in D. mauritiana and D. melanogaster cannot be explained by differences in the amount of proximal heterochromatin. One possible explanation for the reduced centromere effect on these 4 arms might be a substantial increase in the amount of pericentric heterochromatin in *D. mauritiana* that could attenuate the centromere effect relative to *D. melanogaster* by increasing the physical distance between the centromere and the proximal euchromatin. However, careful measures of the genome sizes of these 2 species show that *D. mauritiana* is, in fact, slightly smaller than *D. melanogaster* in terms of genome size (Gregory and Johnston 2008), despite the observation by Chakraborty *et al.* (2021) that the length of euchromatic sequence is greater in *D. mauritiana* than it is in *D. melanogaster*. A greater amount of euchromatic sequence in *D. mauritiana* in the face of a smaller genome size leads to the conclusion that there is less heterochromatin compared with *D. melanogaster*.

To directly test whether a greater amount of pericentric heterochromatin could be the cause of the reduced centromere effect in *D. mauritiana*, we performed DNA fluorescence in situ hybridization (DNA FISH) on mitotic chromosome spreads from *D. melanogaster* and *D. mauritiana* hybrid females. Specifically, we used probes that hybridize with pericentromeric satellite DNA repeats that are abundant in *D. melanogaster* that allow us to identify the species-origin for each mitotic chromosome. Our data clearly show that the *D. melanogaster* chromosomes (arrowheads, Fig. 4, a and b) contain larger DAPI-dense blocks of pericentromeric heterochromatin in comparison to the *D. mauritiana* chromosomes (Fig. 4, a and b). These data suggest that differences in the amount of pericentromeric heterochromatin are unlikely to account for the weakened centromere effect in *D. mauritiana*.

A consideration of exchange frequencies at the level of individual bivalents. The crossover density plots shown in Fig. 3 can only be used to identify where the crossovers occurred, not the arrangement of crossovers on individual bivalents. However, we can obtain such information using the data in Table 1, which presents the primary crossover data in terms of crossover chromatid types (i.e. NCO, SCO, DCO, and TCOs). Because each of these types of chromatids can be obtained from bivalents with a higher number of exchanges (Miller *et al.* 2016), Weinstein (1936) created an algebraic method for characterizing a given population of bivalents in terms of bivalents with no crossovers (E0), 1 crossover event (E1), 2 crossover events (E2), 3 crossover events (E3), and so on. These values are referred to as Exchange Ranks. However, this method can be computationally difficult, especially with small numbers of progeny (Miller *et al.* 2016, 2018). We used a maximum likelihood estimate to derive Weinstein's values. The method is available online at https://simrcompbio.shinyapps.io/CrossoverMLE/.

Results for this analysis are shown in Table 4. We first consider the *3rd* chromosome where in *D. mauritiana*, *3R* displays E2 and E3 frequencies of 0.33 and 0.28 respectively, substantially higher than the values of 0.14 and 0.04, respectively, seen in *D. melanogaster*. A similar high frequency of E3 events can be seen for *3L*. Both *2R* and the *X* display an increased frequency of E2 bivalents in *D. mauritiana*. These increases in bivalents with 1 or more exchange events came at the expense of non-crossover (E0) bivalents. We admit to being impressed by E0 values of zero for *2R*, *3L*, and *3R*. Only on *2L*, the arm on which the centromere effect was unaltered, did *D. mauritiana* show an exchange rank pattern similar to that seen in *D. melanogaster*. Although more complex interpretations are possible, such as arm-specific alterations in the strength of interference, it seems most parsimonious to explain these data as being primarily driven by a reduction in the
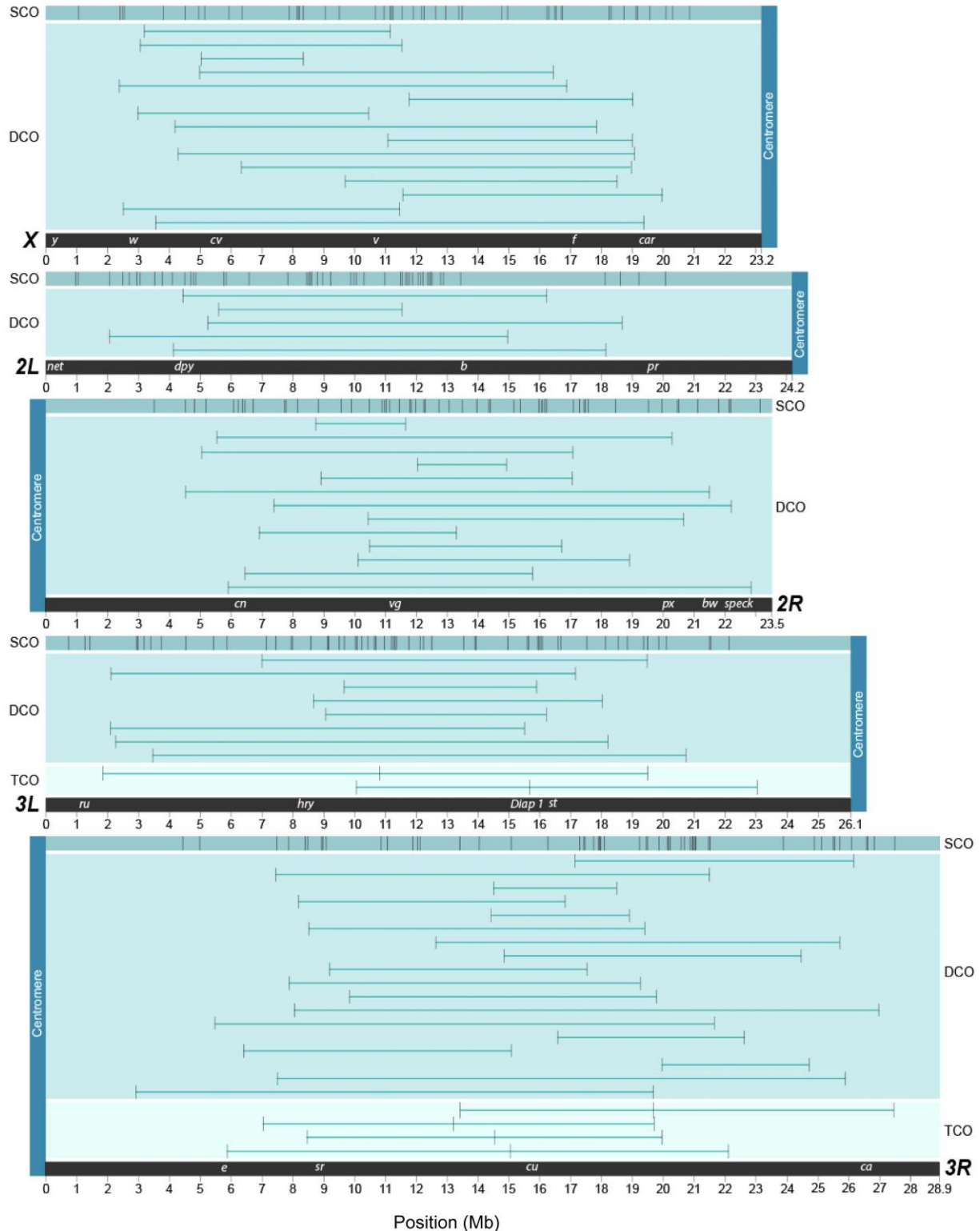
Fig. 2. Crossover positions for the 398 recombinants. Position of the 398 exchange events observed from 105 individual male progeny, where each panel represents 1 of the 5 major *D. mauritiana* chromosome arms (the small 4th chromosome was not examined). The top track in each panel shows the 262 SCO events. The DCO tracks illustrate the locations and spans of 59 DCOs. Six TCO events were identified, 2 on chromosome 3L and 4 on chromosome 3R. That the SCO events making up a DCO or TCO event are well-spaced suggests that interference in *D. mauritiana* is similar to that seen in *D. melanogaster*. Indeed, the average distance between the 2 crossovers that comprise doubles in *D. mauritiana* is 10.6 Mb, which compares well with the value of 10 MB obtained by Miller *et al.* (2016) and suggests that the 2 species do not differ greatly, if at all, in terms of interference.

centromere effect on each arm. This leads to more of each chromosome arm being used for crossovers, resulting in more double, triple, and quadruple exchange events. In support of this hypothesis, we note that our average distance between crossovers on DCO-bearing chromatids is 10.6 MB. This compares well with the value of 10 MB obtained by Miller *et al.* (2016) and suggests

Table 2. Total map lengths in cM (cM per Mb in parentheses).

	Chr 2L	Chr 2R	Chr 3L	Chr 3R	Chr X	Total
Species						
D. mauritiana	57.1 (2.36)	76.2 (3.24)	76.2 (2.91)	96.2 (3.33)	73.3 (3.16)	379.0 (3.01)
D. melanogaster	54.1 (2.30)	51.0 (2.02)	58.1 (2.07)	55.6 (1.73)	57.1 (2.43)	275.9 (2.08)

that the 2 species do not differ greatly, if at all, in terms of interference.

Discussion

We report both a SNP-based map for crossover distribution in *D. mauritiana* and the development of a new and freely available algorithm for determining Weinstein Exchange Ranks using maximum likelihood estimation. At a minimum, our data confirms and extends the work of True *et al.* (1996). However, our ability to position each crossover event along a genome sequence denoting the heterochromatin:euchromatin boundaries of each arm allows the additional conclusions regarding the nature of the centromere effect that are presented below. Specifically, we show that despite reduced amounts of pericentromeric heterochromatin on 4 of the 5 arms of *D. mauritiana* when compared with *D. melanogaster*, the centromere effect on those arms in *D. mauritiana* is much weaker than it is in *D. melanogaster*.

In addition, our ability to detect chromatids bearing double and triple crossovers, and thus determine exchange ranks, allows us to include that the amelioration of the centromere effect on 4 of the 5 chromosome arms increase the euchromatin region available for crossing over and thus provide greater opportunity for double and triple crossovers that might otherwise be precluded by interference.

A new model for the centromere effect: Our data show clearly that reduced heterochromatin on the arms of *D. mauritiana* does not enhance the centromere effect but, paradoxically, is associated with a decrease. In conjunction with prior studies (discussed above) that show a heightened centromere effect when the adjacent pericentromeric heterochromatin is diminished, these data also suggest that the strength of the centromere effect is not related to the simple amount of pericentromeric heterochromatin. We can thus speculate on different models for how the centromere effect is mediated and how this might explain interspecific variation in the genome-wide recombination rate. In 1 model, which could be designated the Inert Spacer Model, the chromatin state *and* sequence of DNA residing between the centromere and regions where recombination is observed have no influence on the centromere effect in any species. Instead, this DNA functions solely as a spacer and DNA of any kind would have the same impact on the centromere effect. Under this model, the centromere effect is primarily mediated by the centromere and genetic factors acting in *trans* with respect to physical distance along the chromosome arm. In a second model, which may be designated the Epigenetic Model, heterochromatin is imbued with a capacity to both limit crossing over within and, more importantly, beyond, in flanking euchromatin. Finally, a third combined model may explain the centromere effect. In this case, the centromere effect is mediated by the centromere and pure physical distance that influence the action of *trans*-acting factors, but the chromatin state and/or sequence composition of DNA between the centromere and heterochromatin modulates the centromere effect.

Studies suggest that a strict epigenetic model for the centromere effect is unlikely. If the mass action of heterochromatin

was the sole cause of the centromere effect, loss of pericentric heterochromatin would lead to either *increased* recombination in regions flanking the deleted heterochromatin (if there was a cumulative repressive effect of bulk heterochromatin) or *no impact* (if a domain of heterochromatin could induce a similar amount of suppression as long as it was sufficient in size). However, neither of these were observed when blocks of pericentric heterochromatin were removed. Rather, deletions of pericentric heterochromatin that bring euchromatin closer to the centromere lead to *lower* rates of recombination in those euchromatic regions (Yamamoto and Miklos 1978). This is consistent with the Inert Spacer Model. But, it does not exclude the possibility that the chromatin state or the DNA sequence composition of pericentric heterochromatin modulates the manner in which the centromere effect is transduced along the chromosome arm.

What explains the ameliorated centromere effect in *D. mauritiana* relative to *D. melanogaster*? Under the Inert Spacer Model, pericentric heterochromatin has no impact on the centromere effect, independent of its functioning as a spacer. Under this model, increased proximal recombination would be explained by increased amounts of spacer pericentric heterochromatin. However, this does not appear to be the case. Since there does not appear to be vastly different amounts of pericentric heterochromatin, a difference in the centromere effect must be explained by differences in centromere structure, differences in *trans*-acting factors that shape the recombination landscape with respect to physical distance from the centromere, differences in the nature of pericentric heterochromatin, which modulates the centromere effect, or a combination of these differences. *Trans*-acting factors may include Mei-352, for which mutations in *D. melanogaster* appear to make crossover frequencies proportional to physical distance, and C(3)G, for which variants increase pericentric recombination (Baker and Carpenter 1972; Page and Hawley 2005; Billmyre *et al.* 2019).

Several observations support the possibility that the evolution of *trans*-acting factors or the centromere itself might contribute to differences in the centromere effect. First, factors that influence meiotic recombination are known to evolve rapidly (Brand *et al.* 2019). Thus, it is likely that factors governing the placement of crossovers with respect to physical distance from the centromere can change in the ways they are influenced by the centromere effect. This is supported by evolutionary observations of *mei-218*. A previous study demonstrated that the replacement of the *D. melanogaster* *mei-218* gene with its *D. mauritiana* counterpart results in an increase in exchange in the proximal euchromatin in *D. melanogaster* (Brand *et al.* 2018). *Mei-218* is very rapidly evolving, with a signature of positive selection, and this rapid evolution appears to have caused a change in the way the centromere impacts recombination. However, as demonstrated by the clear centromere effect observed on *2L* in *D. mauritiana* (see Fig. 3), it cannot be the case that the MEI-218 protein found in *D. mauritiana* cannot impose a centromere effect. In addition to the evolution of these *trans*-acting factors, the evolution of the centromere itself might have an impact. A recent study showed that there has been significant turnover in the sequences that comprise the centromere since the divergence of *D. melanogaster* and *D. mauritiana*
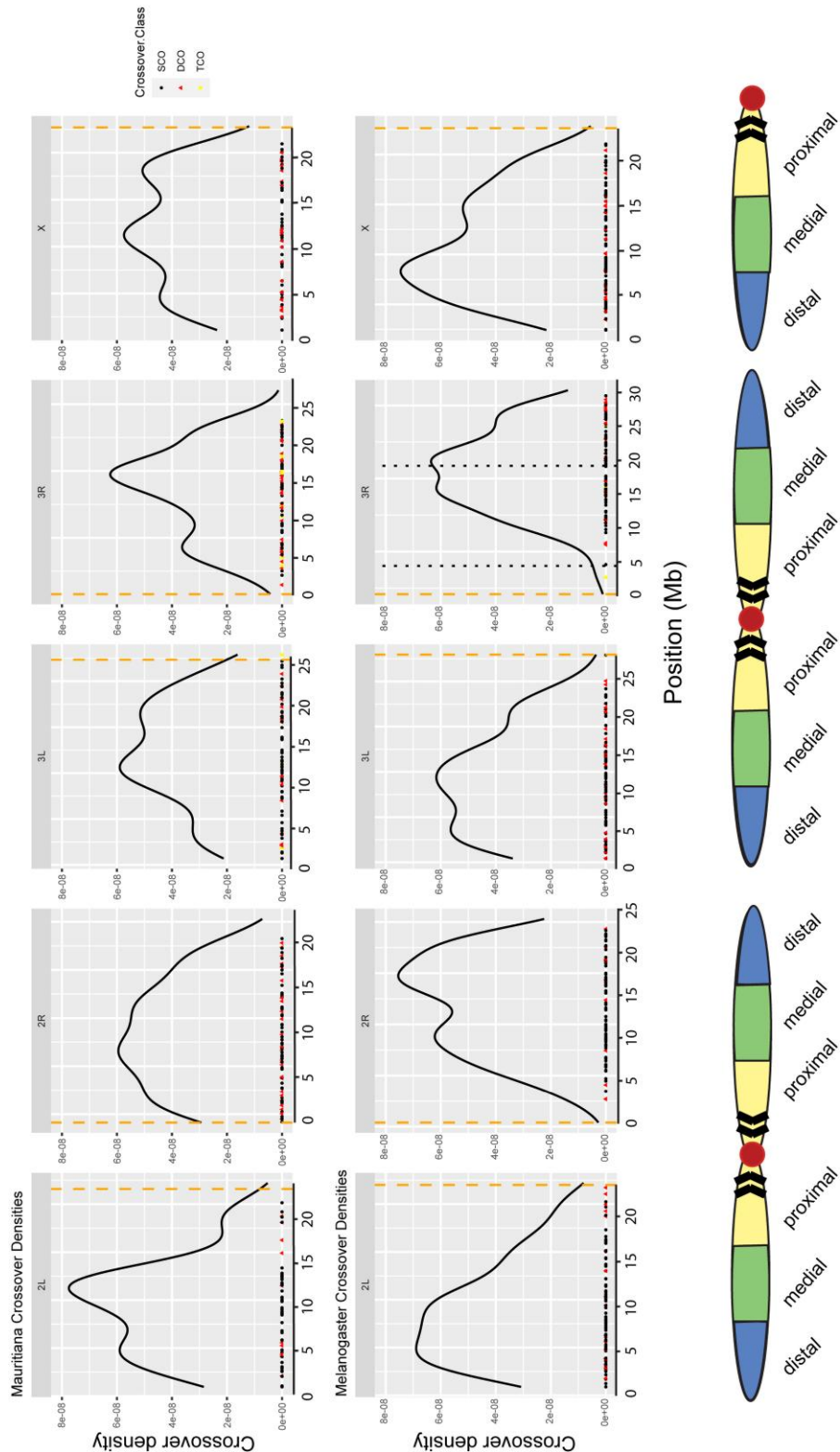
Fig. 3. CO density plots for each of the 5 arms in both *D. mauritiana* and *D. melanogaster*. The euchromatin:heterochromatin boundaries are denoted by dashed yellow lines and the breakpoints of the euchromatic inversion on *3R* are indicated by black dotted lines. The chromosome illustrations indicate the direction of the centromeres in the above plots. Brackets on the chromosomes represent the heterochromatin not included in the plots. *D. melanogaster* data is from Miller *et al.* (2016). Chromosome arms were divided equally into thirds for the proximal, medial, and distal classifications.

(Courret *et al.* 2024). This turnover may lead to a change in the way the centromere shapes proximal meiotic recombination.

Alternatively, while the evolution of *trans*-acting factors and the centromere likely contribute to the amelioration of the *D. mauritiana*

centromere effect, we propose that only some types of heterochromatic regions can buffer the centromere effect, and thus, repeat blocks in the heterochromatin may differ in their ability to attenuate the centromere effect. This is based on several observations. First,

Table 3. Segment CO status.

	Distal 2L			Medial 2L			Proximal 2L			Proximal 2R			Medial 2R			Distal 2R		
	mau	*mel*	P	*mau*	*mel*	P	*mau*	*mel*	P	*mau*	*mel*	P	*mau*	*mel*	P	*mau*	*mel*	P
NCO	82	147		75	155		98	181		87	194		75	153		75	142	
SCO	23	48		30	41		7	15		18	2		28	43		30	53	
DCO	0	1		0	0		0	0		0	0		2	0		0	1	
RF	0.219	0.255	0.760 (0.800)	0.286	0.209	0.073 (0.093)	0.067	0.077	0.632 (0.658)	0.171	0.010	**<0.001 (<0.001)**	0.305	0.219	0.066 (**0.032**)	0.286	0.281	0.468 (0.315)

	Distal 3L			Medial 3L			Proximal 3L			Proximal 3R			Medial 3R			Distal 3R		
	mau	*mel*	P[a]	*mau*	*mel*	P	*mau*	*mel*	P	*mau*	*mel*	P	*mau*	*mel*	P	*mau*	*mel*	P
NCO	83	134		67	149		88	192		83	194		74	146		61	140	
SCO	22	62		35	46		17	4		22	2		29	50		42	55	
DCO	0	0		3	1		0	0		0	0		2	0		2	1	
RF	0.210	0.316	**0.02 (0.050)**	0.390	0.245	**0.008 (0.003)**	0.162	0.020	**<0.001 (<0.001)**	0.210	0.010	**<0.001 (<0.001)**	0.314	0.255	0.156 (0.067)	0.438	0.291	**0.008 (0.001)**

	Distal X			Medial X			Proximal X		
	mau	*mel*	P	*mau*	*mel*	P	*mau*	*mel*	P
NCO	84	163		74	146		80	169	
SCO	21	33		31	48		25	27	
DCO	0	0		0	2		0	0	
RF	0.200	0.168	0.255 (0.238)	0.295	0.265	0.298 (0.275)	0.238	0.138	**0.018 (0.015)**

1/3 segment (Distal, Medial, Proximal) crossover counts for each chromosome arm (2L, 2R, 3L, 3R, and X). P-values were calculated by bootstrapping the segment status 1 million times. P equals the probability, among 1 million random samples, that the recombination frequency in that segment of *D. melanogaster* is higher than the segment in *D. mauritiana*. P-values below in parentheses indicates the same, but normalized for physical distance.
NCO, non-crossover segment; SCO, single crossover segment; DCO, double crossover segment; RF, Recombination frequency.
[a]Indicates a P-value with the hypothesis that the recombination frequency in that segment of *D. mauritiana* is higher than the segment in *D. melanogaster*. Significant P-values are bolded.
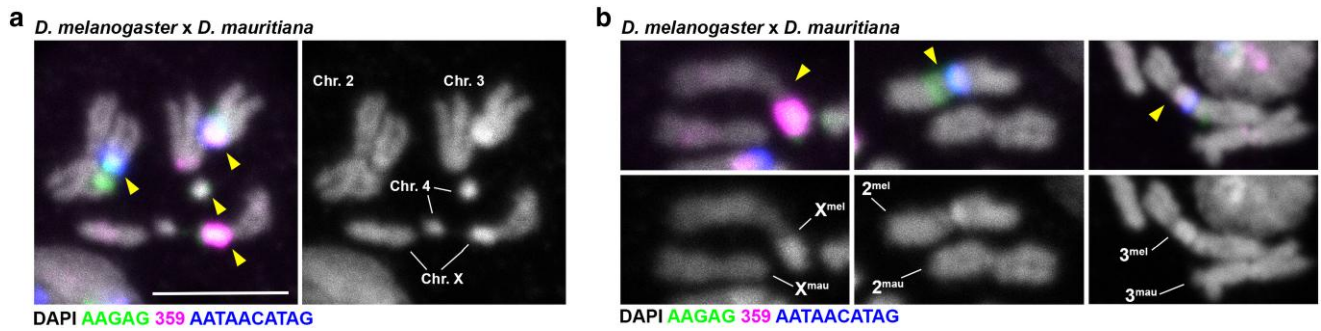
Fig. 4. Cytogenetic comparison of the relative lengths of pericentromeric heterochromatin in *D. melanogaster* and *D. mauritiana* hybrids. a and b) FISH against the $(AATAACATAG)_n$ repeat (blue), the $(AAGAG)_n$ repeat (green), and the 359 bp repeat (magenta) on larval neuroblast mitotic chromosomes from female *D. melanogaster* and *D. mauritiana* hybrids and costained with DAPI (gray). Arrowheads point to *D. melanogaster* chromosomes.

Table 4. MLEs of Weinstein tetrad frequencies.

Exchange rank frequencies	Chr 2L	Chr 2R	Chr 3L	Chr 3R	Chr X
D. mauritiana (this paper)					
E0	0.0476	0.0000	0.0000	0.0000	0.1048
E1	0.7619	0.4903	0.7054	0.3903	0.3238
E2	0.1905	0.5097	0.1607	0.3293	0.5714
E3	0.0000	0.0000	0.1339	0.2804	0.0000
D. melanogaster (Miller et al. 2016.)					
E0	0.1021	0.0815	0.1428	0.1121	0.1224
E1	0.7145	0.8165	0.5511	0.7042	0.6122
E2	0.1835	0.102	0.3061	0.1429	0.2654
E3	0.0000	0.0000	0.0000	0.0408	0.0000

heterochromatin is known to modulate flanking recombination. For example, homozygosity for an inserted fragment of heterochromatin that gives rise to the *brown*^{Dominant} allele suppresses recombination (Slatis 1955), though heterozygosity does not appear to have this effect (Hartmann, Kohl, *et al.* 2019; Hartmann, Umbanhowar, *et al.* 2019). Furthermore, Chakraborty and colleagues demonstrated that one of the most striking differences between the *D. mauritiana* and *D. melanogaster* genomes is the existence of numerous rearrangements within the proximal heterochromatin of the arms (Chakraborty *et al.* 2021). We believe it is likely that these rearrangements influence the impact of the centromere effect. Secondly, Carpenter (1975b, 1975a) demonstrated with serial section electron microscopy that in *D. melanogaster*, the SC has a different morphology in the heterochromatin compared with euchromatin. Since C(3)G can modulate the centromere effect, changes in heterochromatin are likely to influence the centromere effect through the SC (Billmyre *et al.* 2019). Less obvious perturbations in SC structure might also be found in the proximal euchromatin. It will be interesting to see comparative high-resolution studies of SC structure in multiple species within the *melanogaster* complex.

Finally, the exception in proximal region *2L* should be noted. Unlike other proximal regions, the recombination frequency in this region in *D. mauritiana* is actually *less* than what is observed in *D. melanogaster*. If differences in the recombination rate in proximal regions were solely explained by differences in the centromeres or *trans*-acting factors, this exception is difficult to explain. This is especially the case since proximal region *2R* shares a centromere with *2L*, and the recombination rate in *2R*, on the other side of the same centromere, is about 17 times greater in *D. mauritiana*. Thus, if the centromere and *trans*-acting factors explain the difference in *2R*, something must be different about the span of pericentric heterochromatin that maintains significant suppression in *2L* of *D. mauritiana*.

Concluding thoughts: It is perhaps most surprising to us that *D. mauritiana* does not show a centromere effect on 4 of the 5 major arms, but it does show both a level of interference comparable to that observed in *D. melanogaster* and exchange suppression in the telomere adjacent regions. This suggests that changes in the mechanisms that control crossover patterning within a genome (for example, affecting only 4 of the 5 chromosome arms) can alter 1 process, such as the centromere effect, without affecting other processes, such as interference and telomere adjacent suppression. We note in that respect a recent paper showing that the high levels of crossing over and interference observed in budding yeast are not observed in many other species of yeast (Dutta *et al.* 2024). It occurs to us that a proper understanding of the mechanisms that control crossover placement may well require being willing and able to think outside the well-studied model organism box.

Data availability

Acknowledgments

Funding

Conflicts of interest

Literature cited

Baker BS, Carpenter AT. 1972. Genetic analysis of sex chromosomal meiotic mutants in *Drosophilia melanogaster*. Genetics. 71(2): 255–286. https://doi.org/10.1093/genetics/71.2.255.

Barker JSF, Moth JJ. 2001. Linkage maps of *D. simulans*: an update of Sturtevant (1929) with additional loci. Dros Inf Serv. 84:205–206.

Beadle GW. 1932. A possible influence of the spindle fibre on crossing-over in Drosophila. Proc Natl Acad Sci U S A. 18(2): 160–165. https://doi.org/10.1073/pnas.18.2.160.

Berchowitz LE, Copenhaver GP. 2010. Genetic interference: don't stand so close to me. Curr Genomics. 11(2):91–102. https://doi.org/10.2174/138920210790886835.

Billmyre KK, Cahoon CK, Heenan GM, Wesley ER, Yu Z, Unruh JR, Takeo S, Hawley RS. 2019. *X* chromosome and autosomal recombination are differentially sensitive to disruptions in SC maintenance. Proc Natl Acad Sci U S A. 116(43):21641–21650. https://doi.org/10.1073/pnas.1910840116.

Brand CL, Cattani MV, Kingan SB, Landeen EL, Presgraves DC. 2018. Molecular evolution at a meiosis gene mediates species differences in the rate and patterning of recombination. Curr Biol. 28(8):1289–1295.e4. https://doi.org/10.1016/j.cub.2018.02.056.

Brand CL, Wright L, Presgraves DC. 2019. Positive selection and functional divergence at meiosis genes that mediate crossing over across the Drosophila phylogeny. G3 (Bethesda). 9(10):3201–3211. https://doi.org/10.1534/g3.119.400280.

Carpenter AT. 1975a. Electron microscopy of meiosis in *Drosophila melanogaster* females. I. Structure, arrangement, and temporal change of the synaptonemal complex in wild-type. Chromosoma. 51(2): 157–182. https://doi.org/10.1007/bf00319833.

Carpenter AT. 1975b. Electron microscopy of meiosis in *Drosophila melanogaster* females: II. The recombination nodule–a recombination-associated structure at pachytene? Proc Natl Acad Sci U S A. 72(8):3186–3189. https://doi.org/10.1073/pnas.72.8.3186.

Carpenter AT, Sandler L. 1974. On recombination-defective meiotic mutants in *Drosophila melanogaster*. Genetics. 76(3):453–475. https://doi.org/10.1093/genetics/76.3.453.

Cattani MV, Kingan SB, Presgraves DC. 2012. Cis- and trans-acting genetic factors contribute to heterogeneity in the rate of crossing over between the *Drosophila simulans* clade species. J Evol Biol. 25(10):2014–2022. https://doi.org/10.1111/j.1420-9101.2012.02578.x.

Chakraborty M, Chang CH, Khost DE, Vedanayagam J, Adrion JR, Liao Y, Montooth KL, Meiklejohn CD, Larracuente AM, Emerson JJ. 2021. Evolution of genome structure in the *Drosophila simulans* species complex. Genome Res. 31(3):380–396. https://doi.org/10.1101/gr.263442.120.

Courret C, Hemmer LW, Wei X, Patel PD, Chabot BJ, Fuda NJ, Geng X, Chang CH, Mellone BG, Larracuente AM. 2024. Turnover of retroelements and satellite DNA drives centromere reorganization over short evolutionary timescales in Drosophila. PLoS Biol. 22(11): e3002911. https://doi.org/10.1371/journal.pbio.3002911.

Dutta A, Dutreux F, Garin M, Caradec C, Friedrich A, Brach G, Thiele P, Gaudin M, Llorente B, Schacherer J. 2024. Multiple independent losses of crossover interference during yeast evolutionary history. PLoS Genet. 20(9):e1011426. https://doi.org/10.1371/journal.pgen.1011426.

Garrigan D, Kingan SB, Geneva AJ, Vedanayagam JP, Presgraves DC. 2014. Genome diversity and divergence in *Drosophila mauritiana*: multiple signatures of faster X evolution. Genome Biol Evol. 6(9):2444–2458. https://doi.org/10.1093/gbe/evu198.

Gregory T, Johnston JS. 2008. Genome size diversity in the family Drosophilidae. Heredity (Edinb). 101(3):228–238. https://doi.org/10.1038/hdy.2008.49.

Hartmann M, Kohl KP, Sekelsky J, Hatkevich T. 2019. Meiotic MCM proteins promote and inhibit crossovers during meiotic recombination. Genetics. 212(2):461–468. https://doi.org/10.1534/genetics.119.302221.

Hartmann M, Umbanhowar J, Sekelsky J. 2019. Centromere-proximal meiotic crossovers in *Drosophila melanogaster* are suppressed by both highly repetitive heterochromatin and proximity to the centromere. Genetics. 213(1):113–125. https://doi.org/10.1534/genetics.119.302509.

Hatkevich T, Kohl KP, McMahan S, Hartmann MA, Williams AM, Sekelsky J. 2016. Bloom syndrome helicase promotes meiotic crossover patterning and homolog disjunction. Curr Biol. 27(1): 96–102. https://doi.org/10.1016/j.cub.2016.10.055.

Hawley RS. 1980. Chromosomal sites necessary for normal levels of meiotic recombination in *Drosophila melanogaster*. I. Evidence for and mapping of the sites. Genetics. 94(3):625–646. https://doi.org/10.1093/genetics/94.3.625.

Jagannathan M, Warsinger-Pepe N, Watase GJ, Yamashita YM. 2017. Comparative analysis of satellite DNA in the *Drosophila melanogaster* species complex. G3 (Bethesda). 7(2):693–704. https://doi.org/10.1534/g3.116.035352.

Kohl KP, Jones CD, Sekelsky J. 2012. Evolution of an MCM complex in flies that promotes meiotic crossovers by blocking BLM helicase. Science. 338(6112):1363–1365. https://doi.org/10.1126/science.1228190.

Larracuente AM, Ferree PM. 2015. Simple method for fluorescence DNA in situ hybridization to squashed chromosomes. J Vis Exp. 95:52288. https://doi.org/10.3791/52288.

Lindsley DL, Sandler L. 1977. The genetic analysis of meiosis in female *Drosophila melanogaster*. Philos Trans R Soc Lond B Biol Sci. 277(955):295–312. https://doi.org/10.1098/rstb.1977.0019.

Mehrotra S, McKim KS. 2006. Temporal analysis of meiotic DNA double-strand break formation and repair in Drosophila females. PLoS Genet. 2(11):e200. https://doi.org/10.1371/journal.pgen.0020200.

Miller DE, Smith CB, Kazemi NY, Cockrell AJ, Arvanitakis AV, Blumenstiel JP, Jaspersen SL, Hawley RS. 2016. Whole-Genome analysis of individual meiotic events in *Drosophila melanogaster* reveals that noncrossover gene conversions are insensitive to interference and the centromere effect. Genetics. 203(1):159–171. https://doi.org/10.1534/genetics.115.186486.

Miller DE, Staber C, Zeitlinger J, Hawley RS. 2018. Highly contiguous genome assemblies of 15 Drosophila species generated using nanopore sequencing. G3 (Bethesda). 8(10):3131–3141. https://doi.org/10.1534/g3.118.200160.

Page SL, Hawley RS. 2005. The Drosophila meiotic mutant *mei-352* is an allele of *klp3A* and reveals a role for a kinesin-like protein in crossover distribution. Genetics. 170(4):1797–1807. https://doi.org/10.1534/genetics.105.041194.

Pazhayam NM, Frazier LK, Sekelsky J. 2024. Centromere-proximal suppression of meiotic crossovers in Drosophila is robust to changes in centromere number, repetitive DNA content, and

centromere-clustering. Genetics. 226(3):iyad216. https://doi.org/10.1093/genetics/iyad216.

Pazhayam NM, Sagar S, Sekelsky J. 2025. Suppression of meiotic crossovers in pericentromeric heterochromatin requires synaptonemal complex and meiotic recombination factors in Drosophila melanogaster [preprint]. Genetics. https://doi.org/10.1093/genetics/iyaf029

Pazhayam NM, Turcotte CA, Sekelsky J. 2021. Meiotic crossover patterning. Front Cell Dev Biol. 9:681123. https://doi.org/10.3389/fcell.2021.681123.

Pettie N, Llopart A, Comeron JM. 2022. Meiotic, genomic and evolutionary properties of crossover distribution in *Drosophila yakuba*. PLoS Genet. 18(3):e1010087. https://doi.org/10.1371/journal.pgen.1010087.

Robinson JT, Thorvaldsdóttir H, Winckler W, Guttman M, Lander ES, Getz G, Mesirov JP. 2011. Integrative genomics viewer. Nat Biotechnol. 29(1):24–26. https://doi.org/10.1038/nbt.1754.

Schalet A, LeFevre G Jr. 1976. The proximal region of the X chromosome. In: Ashburner M, Novitski E, editors. Genetics and biology of Drosophila. London: Academic Press. p. 847–902 1b.

Slatis HM. 1955. A reconsideration of the brown-dominant position effect. Genetics. 40(2):246–251. https://doi.org/10.1093/genetics/40.2.246.

Sturtevant AH. 1913. A third group of linked genes in *Drosophila ampelophila*. Science. 37(965):990–992. https://doi.org/10.1126/science.37.965.990.

Sturtevant AH. 1915. The behavior of the chromosomes as studied through linkage. Z Indukt Abstamm Vererbungsl. 13(1):234–287. https://doi.org/10.1007/BF01792906.

Sturtevant AH, Beadle GW. 1936. The relations of inversions in the X chromosome of Drosophila melanogaster to crossing over and disjunction. Genetics. 21(5):554–604. https://doi.org/10.1093/genetics/21.5.554.

Szauter P. 1984. An analysis of regional constraints on exchange in *Drosophila melanogaster* using recombination-defective meiotic mutants. Genetics. 106(1):45–71. https://doi.org/10.1093/genetics/106.1.45.

True JR, Mercer JM, Laurie CC. 1996. Differences in crossover frequency and distribution among three sibling species of Drosophila. Genetics. 142(2):507–523. https://doi.org/10.1093/genetics/142.2.507.

Weinstein A. 1936. The theory of multiple-strand crossing over. Genetics. 21(3):155–199. https://doi.org/10.1093/genetics/21.3.155.

Yamamoto M, Miklos GL. 1977. Genetic dissection of heterochromatin in Drosophila: the role of basal X heterochromatin in meiotic sex chromosome behaviour. Chromosoma. 60(3):283–296. https://doi.org/10.1007/bf00329776.

Yamamoto M, Miklos GL. 1978. Genetic studies on heterochromatin in *Drosophila melanogaster* and their implications for the functions of satellite DNA. Chromosoma. 66(1):71–98. https://doi.org/10.1007/BF00285817.

Zwick ME, Cutler DJ, Langley CH. 1999. Classic Weinstein: tetrad analysis, genetic variation and achiasmate segregation in Drosophila and humans. Genetics. 152(4):1615–1629. https://doi.org/10.1093/genetics/152.4.1615.

Editor: A. MacQueen